

Hydrothermally stable molecular separation membranes from organically linked silica

R. Kreiter

J.F. Vente

H.L. Castricum (MESA+ Institute for Nanotechnology)

A. Sah (MESA+ Institute for Nanotechnology)

D.H.A. Blank (MESA+ Institute for Nanotechnology)

J.E. ten Elshof (MESA+ Institute for Nanotechnology)

Published in Journal of Materials Chemistry, 2008, 18, 2150-2158

DOI: 10.1039/b801972j

ECN-W--08-028 JUNE 2008

Hydrothermally stable molecular separation membranes from organically linked silica†

Hessel L. Castricum, *ab Ashima Sah, *a Robert Kreiter, *b Dave H. A. Blank, *a Jaap F. Vente* and Johan E. ten Elshof *a*

Received 4th February 2008, Accepted 4th March 2008
First published as an Advance Article on the web 14th March 2008
DOI: 10.1039/b801972j

A highly hydrothermally stable microporous network material has been developed that can be applied in energy-efficient molecular sieving. The material was synthesized by employing organically bridged monomers in acid-catalysed sol-gel hydrolysis and condensation, and is composed of covalently bonded organic and inorganic moieties. Due to its hybrid nature, it withstands higher temperatures than organic polymers and exhibits high solvolytical and acid stability. A thin film membrane that was prepared with the hybrid material was found to be stable in the dehydration of n-butanol at 150 °C for almost two years. This membrane is the first that combines a high resistance against water at elevated temperatures with a high separation factor and permeance. It therefore has high potential for energy-efficient molecular separation under industrial conditions, including the dehydration of organic solvents. The organically bridged monomers induce increased toughness in the thin film layer. This suppresses hydrolysis of Si-O-Si network bonds and results in a high resistance towards stress-induced cracking. The large non-hydrolysable units thus remain well incorporated in the surrounding matrix such that the material combines high (pore) structural and mechanical stability. The sol mean particle size was found to be a viable parameter to tune the thickness of the membrane layer and thus optimize the separation performance. We anticipate that other hybrid organosilicas can be made in a similar fashion, to yield a whole new class of materials with superior molecular sieving properties and high hydrothermal stability.

1. Introduction

Nanostructured membranes¹⁻³ are expected to play a key role in meeting the energy demands of the future.⁴ Energy-efficient separation of biomass fuels⁵ and of hydrogen⁶ are examples of membrane applications in upcoming technologies for green energy production. Further applications can be found in the replacement of energy-consuming processes, especially breaking azeotropic mixtures during distillation and dehydration of condensation reactions.⁷ However, large-scale industrial usage of membranes will only become economically feasible when they can be operated at elevated temperatures for several years. This is related to the typical temperature of many process streams, as well as to the high cost of module replacement and concomitant process discontinuation.⁸

The state-of-the-art ceramic membrane for molecular separation of gases and liquids is a layered hierarchical porous support system with a selective 30–100 nm thin film of nanoporous silica (SiO₂). The suitability of this material for molecular separations originates from the fact that it can be moulded into an amorphous, glassy film with pore diameters between 2 and 4 Å, similar to the kinetic diameter of small molecules. Silica membranes combine a high permeability for small molecules such as water (kinetic diameter 2.6 Å⁹) and hydrogen (2.9 Å) with a very low permeability for larger molecules ($>\sim$ 3 Å). The amorphous silica nanostructure consists of randomly connected SiO₄ tetrahedra, and can be applied in dry gas atmospheres up to about 600 °C.10 However, it lacks microstructural stability in the presence of water at temperatures as low as 60 °C.11 Prolonged exposure to water gives the net reaction ≡Si-O-Si≡ + H₂O → 2 ≡Si-OH and results in the release of silica moieties from high energy sites near nanopores to lower energy sites elsewhere in the material. As a result, dense particles with large nonselective pores are formed.12 These larger pores can be considered as defects and impair the functionality of the membrane.

Several strategies have been proposed to improve membrane durability. The first strategy is to employ metal oxides with more stable M–O bonds, such as TiO₂ or ZrO₂. Unfortunately, they tend to crystallize in the presence of water even at low temperatures, ¹¹ resulting in a discontinuous structure with substantially larger pores. To our best knowledge, no pure defect-free ZrO₂ or TiO₂ membrane with molecular separation potential based on nanopore structure has been synthesised,

^aInorganic Materials Science, MESA+ Institute for Nanotechnology, University of Twente, P.O. Box 217, 7500 AE Enschede, The Netherlands. E-mail: j.e.tenelshof@utwente.nl; Fax: (+31) 53 4893595; Tel: (+31) 53 4892695

^bVan't Hoff Institute for Molecular Sciences, University of Amsterdam, Nieuwe Achtergracht 166, 1018 WV Amsterdam, The Netherlands. E-mail: castric@science.uva.nl; Fax: (+31) 20 5255601; Tel: (+31) 20 5256493

^cEnergy Research Centre of the Netherlands, Postbus 1, 1755 ZG Petten, The Netherlands; Fax: (+31) 224 568615; Tel: (+31) 224 564949

[†] Electronic supplementary information (ESI) available: SAXS patterns of sols I–III and a N₂ adsorption isotherm of an unsupported film from sol II. See DOI: 10.1039/b801972j

but promising properties were found for a microporous (Zr/Ti)O₂ composite material.¹³ The second approach is to replace the amorphous silica network by a crystalline network as found in zeolites.^{3,14} Zeolites are known to have excellent permselectivities. It is however challenging to grow them into ultrathin layers and stability limitations exist as well. For instance, zeolite A can only be operated under very limited and specific conditions, as the mixture should be free of Ca ions¹⁵ and the pH window is limited to between 6.5 and 7.5.¹⁶ Most other zeolites have channel sizes too large for size-based molecular sieving of small molecules like H₂ or H₂O. Whereas zeolites can thus be used very well in specific applications, new membrane materials are still required for molecular separations under more inhospitable operating conditions.

A third strategy is the incorporation of hydrolytically stable groups with hydrophobic character to protect the siloxane bonds by shielding them from water. Owing to the inaccessibility of the nanopores for organic molecules, the SiO2-based matrix including any hydrophobic entities has to be assembled in a one-pot synthesis. This can be achieved by employing the versatile and mild processing conditions of sol-gel synthesis. Typically, alkoxysilane precursors $Si(OR)_4$ and $R'-Si(OR)_3$ are used, where R represents an alkyl group and R' is a functional (non-reactive) side group. The alkoxy group OR leaves the precursor after exchange with water (hydrolysis), thus permitting condensation of the resulting ≡Si-OH groups into siloxane bonds and finally leading to the formation of an inorganic network. Improved hydrothermal stability was obtained by the incorporation of hydrophobic -CH₃ groups into silica by co-condensation of Si(OEt)₄ (TEOS) and CH₃-Si(OEt)₃ (MTES). 17,18 Water transport was not impaired by the introduction of the organic groups. Other advantages of this strategy are that very thin layers can be prepared, which is required for high permeabilities, and that amorphous silica is insensitive to the presence of bivalent ions. However, the concentration of alkyl groups that could be introduced in this way was limited to a CH_x: Si molar ratio of 0.5, and only moderate improvement of durability was achieved.

The concept of the present work is to replace as many siloxane bonds as possible by hydrolytically stable Si-C links, thus introducing a new nanoporous network to membrane technology. The material resembles periodic mesoporous organosilicas (PMOs)¹⁹ with mesopores >2 nm which have been prepared in bulk form from similar precursors that were originally introduced by Loy and Shea.20,21 However, PMOs have no molecular sieving properties. The hybrid material that we developed has a fully amorphous organic/inorganic nanoporous network structure and can be prepared in the form of a supported thin layer by using a bridged bis-silyl precursor, (EtO)₃Si-CH₂CH₂-Si(OEt)₃ (BTESE). The concomitant effect is that the CH_x: Si molar ratio is raised to unity. Recently, we reported the excellent stability of a material prepared from this precursor in molecular separation.²² Here, we describe in detail the various processing stages that result in a defect-free selective membrane layer. This includes engineering of the sol particle size and morphology, characterisation of the porous structure with different molecular probes, and membrane testing. We applied dehydration by pervaporation to compare its performance to earlier amorphous inorganic membrane generations. Enhanced

stability in dehydration would concomitantly give good prospects for a wealth of separations in which water is a minor component. We tested the performance both with respect to selectivity towards molecular transport and to long-term stability under realistic process conditions.

2. Experimental

2.1. Material preparation

1,2-Bis(triethoxysilyl)ethane (BTESE, purity 96%, Aldrich) was distilled before use at 1 bar to remove traces of impurities and water, and mixed with an equal molar amount of methyltriethoxysilane (MTES, purity 99%, Aldrich). This mixture was subsequently diluted with dry ethanol in an ice bath. The required amounts of distilled water and nitric acid (65 wt%, Aldrich) were mixed and added dropwise to the precursor mixture under continuous stirring. Half of the total amount of water was added at the beginning, the other half after 90 min of refluxing. Water addition took place after placing the mixture (or sol) in an ice bath. Subsequently, the sol was allowed to reflux at 60 °C. The mixtures had a [H⁺]: [silane] ratio of 0.1 and [H₂O]: [–OEt] ratios as reported in Table 1, at [Si] = 1.8 M. Unsupported films were obtained by drying the sols in a Petri dish. The size of the film parts was reduced to several mm for further analysis.

Disk-shaped and tubular supported γ -alumina membranes were dip-coated with freshly prepared hybrid silica sol. The support consisted of a mesoporous γ -alumina layer 10,23 which was deposited on an α -alumina support system as described by Bonekamp. 24 The silica sol was coated onto this layer under class 1000 cleanroom conditions to prevent defect formation due to dust particles. The supported and unsupported films were thermally treated at 300 °C for 3 h in a N_2 flow (99.999% pure) with 0.5 °C min $^{-1}$ heating and cooling rates.

2.2. Sol characterization

²⁹Si Nuclear magnetic resonance spectra on sols were acquired at 213 K on a Bruker 500 MHz NMR and referenced to tetramethylsilane. Pulse duration was 10 μs (~45° pulse), with a repetition rate of 2.5 s. Tris(acetylacetonato)chromium(III) (0.1 wt%) was added to increase the demagnetization rate of the silicon nucleus. Condensation (Si–O–Si bond formation) was observed by a 10 ppm upfield shift of the signal. Colloid sizes in the freshly prepared sols were determined in a 25% dilution in EtOH by dynamic light scattering (DLS) at 25 °C in a Malvern Zetasizer Nano.

Small-angle X-ray scattering (SAXS) measurements were performed at the DUBBLE beamline BM-26B²⁵ of the European

Table 1 Analytical data for hybrid sols and membranes: hydrolysis ratio, mean sol particle size and sol fractal dimension, membrane layer thickness and permeate water content from a 95% n-butanol-5% water mixture at 95 °C

	Sol			Membrane		
	$[H_2O]:[OEt]$	$d_{\rm sol}$ /nm	$D_{ m f}$	Thickness/μm	% H ₂ O	
I	0.5	2.2	0.6	0.03	30	
II	1	4.9	1.1	0.12	94	
III	2	13	1.4	1.5		

Synchrotron Radiation Facility in Grenoble, France. Scattering data were obtained at an X-ray beam energy of 12 keV. After background subtraction, the fractal dimension $D_{\rm f}$ was determined from an exponential fit of the intensity $I \sim {\rm e}^{-D_{\rm f}}$.

2.3. Solid characterization

Thermogravimetric analysis–mass spectrometry (TGA-MS) was carried out in a Setaram TG 85 thermobalance in Ar (99.999% pure) and synthetic air (20% O_2 in N_2 , 99.999% purity). The reaction products were analyzed for carbon-containing molecules with a Pfeiffer QMS 200 mass spectrometer (m/z range 0–200) equipped with a ChanneltronTM detector.

Adsorption/desorption isotherms on dried ($p < 10^{-4}$ mbar at 473 K) thermally treated unsupported films were determined at 77 K (N₂) and 273 K (CO₂, C₂H₂) on a CE-Instruments Milestone 200. Surface areas were determined from the adsorption isotherms by the Dubinin method, modified by Kaganer,²⁶ represented by $\log n = \log n_{\rm m} + D(\log p^0/p)^2$, with n the gas adsorbed at relative pressure p/p^0 , $n_{\rm m}$ the monolayer capacity of the surface, both in mol per g adsorbent, and D an adsorbate-dependent constant. The molecular surface areas were taken as 0.162 nm² for N₂, 0.179 nm² for CO₂ and 0.204 nm² for C₂H₂. The solid skeletal (network) density was determined by gas pycnometry at room temperature, with He as a replacement gas, in a Multivolume Pycnometer 1305 after the same drying procedure.

Fourier-transform infra-red (FTIR) spectroscopy was performed on dried unsupported films, using a diffuse reflectance infrared Fourier transform cell in a Bio-Rad FT175 at room temperature.

Chemical stability of the unsupported films was assessed by soaking 0.11 g of powdered material in 10 ml of aqueous solutions of nitric acid or sodium hydroxide. The pH was varied between 1.5 and 13 and the solid was left in the liquid at room temperature for 24 h. The Si concentration was then assessed by atomic adsorption spectroscopy (AAS, Unicam Spectra AA 939, Solaar), using a nitrous oxide–acetylene gas mixture.

2.4. Membrane characterization

High resolution scanning electron microscopy (SEM) was carried out on a LEO Gemini 1550 FEG-SEM at a voltage of $0.60\ kV$.

XPS was carried out with a PHI Quantera Scanning ESCA microprobe with an analysis depth of 5–75 Å. Depth profiles of the concentrations of Si and Al inside the membrane were obtained from the Si 2p and Al 2p energy bands by sputtering with 3 keV Ar⁺ at 24 nm min⁻¹.

Permporometry was carried out with water vapour as the condensable gas and He as the diffusional gas²⁷ at a temperature of 150 °C. A pressure gradient was applied such that helium transport occurred by molecular diffusion and pressure-driven transport. The Kelvin equation was extrapolated to values in the microporous range below 2 nm to approximate the pore size distribution.

Pervaporation of *n*-butanol-water mixtures over the membranes was carried out in a stirred vessel at 95 °C (95 : 5 wt% *n*-butanol-water, 1 bar) and in a stirred stainless steel

autoclave at 150 $^{\circ}$ C (5 bar). The permeate side of the membrane was kept at 10 mbar with a vacuum pump. For determining steady-state flux and selectivity, the vapours were collected at the permeate side in a liquid nitrogen-based cold trap and the weight increase measured with an electronic balance. The compositions of the feed and the permeate were determined by Karl Fischer titrations.

3. Results

3.1. Sol structure engineering

A challenge in the preparation of a homogeneous thin layer using BTESE was to avoid the formation of cyclic carbosiloxane structures. These have been reported to slow and even completely shut down gelation and therefore are not incorporated in a continuous network structure.21 To lower the statistical chance of formation of the inert cyclic structures, we added a substantial fraction of MTES at an early stage of sol preparation. In this way, we could minimize auto-condensation of BTESE and maximize co-condensation, and at the same time profit from the incorporation of shielding CH₃ groups.¹⁷ Firstly, we had to ensure that the reaction rates of MTES and BTESE were of the same order of magnitude. By monitoring with ²⁹Si solution NMR, we found only 1.3 times faster condensation (Si-O-Si bond formation) for MTES. The condensation rates are thus sufficiently similar to suppress auto-condensation of BTESE. The slightly faster condensation kinetics of MTES can be explained by steric and electronic effects related to its (twice) smaller size and somewhat different electronic charge distribution.

The parallel approach to maximize co-condensation was by moderating the high silane reactivity to hydrolysis. We controlled this highly exothermic hydrolysis step by employing water-lean conditions and by mixing the reactants in an ice bath. This allows homogeneous development of a sol with only a small number of bonds formed in the earliest stages. Gradual bond formation promotes the development of an open fractal polymer, which is required for obtaining a suitable percolative structure with molecular-sieving ability.²⁸ To allow full development of the sol, subsequent water additions were required. Water was thus supplied in phases to the reaction mixture. The growth rate was found to be related to the total amount of water added to the sample. This means that the size of the sol particles could be tuned by adapting the total amount of added water.

We studied three sol recipes with different hydrolysis ratios, *i.e.* the ratio between the number of water molecules and the number of reactive ethoxy groups (Table 1). All other reaction conditions were kept constant. The sol colloid size distributions are shown in Fig. 1. The sols were prepared under acidic conditions, which are needed to form microporous structures.²⁹ The sol particle sizes were characterized with DLS, while small angle X-ray scattering was applied to obtain the fractal dimension (*i.e.*, the degree to which the inorganic polymer has a branched structure within the sol particles). The hydrolysis ratio was found to have a considerable effect on the colloid size distribution and the connectivity (Table 1). For all sols the size distribution of the colloids was quite broad. A more than double mean diameter was found for a doubled hydrolysis ratio. A hydrolysis ratio

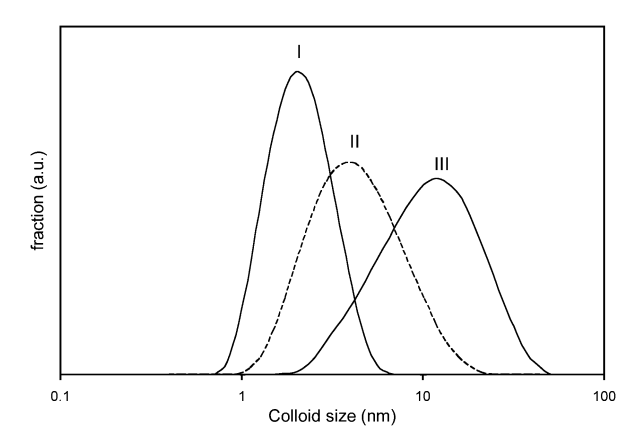


Fig. 1 Sol colloid size distributions determined by dynamic light scattering. After initial reaction under water-lean conditions, more water was added to obtain sols with final hydrolysis ratios $[H_2O]$: [-OEt] of 0.5 (I), 1 (II, dashed) and 2 (III).

larger than 2 resulted in highly viscous gels, which were unsuitable for the dip-coating procedure applied for membrane preparation. The fractal dimension defines the final structure of the solid inorganic polymer network. Sols with fractal dimensions below 1.5 are known to result in microporous solid materials.^{28,30} Acid-catalysed condensation is needed to obtain colloidal particles that are constituted of polymeric chains with limited branching. A fractal dimension <1.5 allows interpenetration of these polymer chains upon drying, resulting in a fully microporous material. Colloids with a fractal dimension higher than 1.5 would rather result in mesoporous structures due to 'hard sphere packing', with pores on the order of the colloid size. A maximum fractal dimension of 1.5 is thus a strict requirement for obtaining a network with a percolative structure and pores <2 nm. All three investigated sols had fractal dimensions below this value, and were thus expected to evolve into microporous solid materials.

3.2. Thermal and chemical stability

Unsupported films were prepared from sols I-III by drying them in a Petri dish followed by structural consolidation of the formed gels by a heat treatment at 300 °C in nitrogen. By FTIR spectroscopy we confirmed the presence of organic moieties in the unsupported films. The analysis indicated a well-connected structure without liquid or adsorbed ethanol remaining from the preparation procedure. The symmetric and asymmetric stretching of the C–H bonds of the organic groups can be found in the high-frequency range (Fig. 2). We found that the spectrum of the BTESE-MTES mixture can be explained very well by superposition of the spectra of the pure components. MTESbased gels can be identified by a characteristic peak at 2975 cm⁻¹.31 This was also found in mixed TEOS-MTES gels that were used for the preparation of methylated silica membranes. BTESE-based gels are characterized by a peak at 2800 cm⁻¹ and a much broader feature between 2875 and 2950 cm⁻¹. The spectrum of purely inorganic SiO₂ films prepared from TEOS is completely featureless in this range. The spectrum thus shows the persistence of both methyl and -CH₂-CH₂- groups in the film after the consolidation treatment. The thermal stability of the materials was confirmed with TGA-MS (Fig. 3). Below

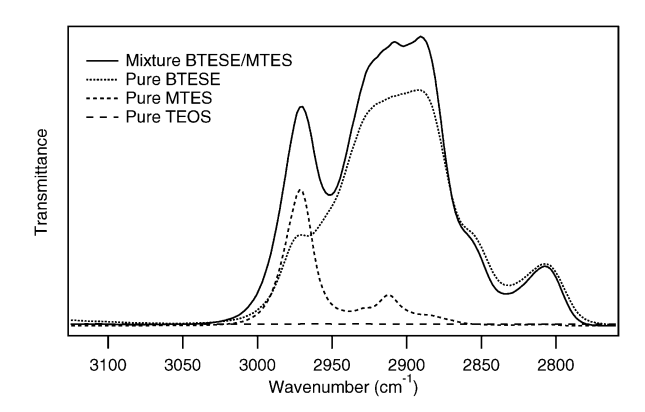


Fig. 2 FTIR spectrum of thermally treated unsupported hybrid films ('mixture'), compared with those of films prepared from TEOS, MTES and BTESE.

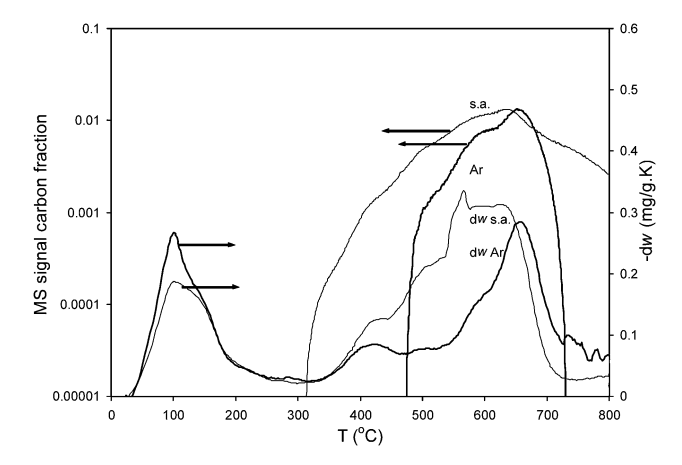


Fig. 3 Differential weight traces of thermally treated unsupported hybrid films measured with TGA (right axis), and MS signal of carbon-containing fragments (left axis) during heating in argon (Ar, thick lines) and in synthetic air (s.a., thin lines).

470 °C, the weight loss in an inert (argon) atmosphere could entirely be attributed to water evolution due to dehydration and dehydroxylation. Only above this temperature decomposition of organic groups was observed. Even in an oxidative atmosphere, the material was found to be thermally stable up to 315 °C. We thus established that the solid had remained a truly organic—inorganic hybrid network material after a non-oxidative thermal treatment at 300 °C.

Chemical stability of the hybrid films was assessed from the amount of Si leached into a liquid phase at room temperature, as determined by AAS. Table 2 gives the wt% of Si present in a fixed volume after treatment with solutions of different pH. We found very little dissolution of the hybrid powders in acid conditions down to a pH of 1.5, with silicon concentrations below the detection limit. In basic solutions, chemical stability is much lower. The pH stability follows the trend for purely

Table 2 Chemical stability of thermally treated hybrid films at various acid/base strengths

pH	1.5–5.5	6.5	8.5	11.5	13.0
Leached into solution (wt% Si)	< 0.006	0.07	0.3	0.8	1.0

inorganic silica,³² and is likely determined by the specific chemical stability of the siloxane bonds. Similar tests with a range of organic solvents, including DMF, THF and hexane, showed no leaching or swelling.

3.3. Nanopore characterisation

We assessed the pore structure of the three solid unsupported films by vapour adsorption, employing different molecular probes. We found large differences between the surface areas determined from the adsorption isotherms (Table 3). High values were found with CO₂ and C₂H₂, but zero surface area was determined with N2. Even at the relatively high temperature (273 K) applied for CO₂ and C₂H₂ adsorption, equilibration times were very long. Clearly, the pores were so small that molecular transport remained sluggish even considering the enhanced kinetics at this temperature. From the diameters of the different molecules, it follows that the average diameter of nanopores is close to 0.24 nm, and that virtually all pores are less than 0.3 nm wide. The surface areas of the various unsupported films differ only slightly. All three unsupported films exhibited a narrow pore size distribution with very small pores. Taking the sizes of the molecular probes into consideration, the pores of the three unsupported thermally treated hybrid silica films were found to be somewhat smaller than in inorganic and methylated silica.33

The higher skeletal density of the BTESE–MTES unsupported films, determined with helium pycnometry, indicated fewer inaccessible pores than in a pure MTES-based film (1.3 g ml⁻¹).³³ As the materials have the same gross organic fraction, they can be expected to have similar skeletal densities, and the difference should thus be ascribed to a greater volume inaccessible to He in methylated silica. Pore filling by diffusing He was very slow, up to several minutes at room temperature, which is indicative of the presence of pores with a diameter close to the size of He (0.20 nm). This agrees with the small pore size found with adsorption techniques.

Thus, at the same organic fraction, we created a series of materials with a narrower pore size distribution and higher effective adsorption capability of very small molecules than

Table 3 Surface areas determined from adsorption isotherms with various molecular probes, and skeletal densities determined with He pycnometry. The sizes of the molecular probes are indicated in parentheses

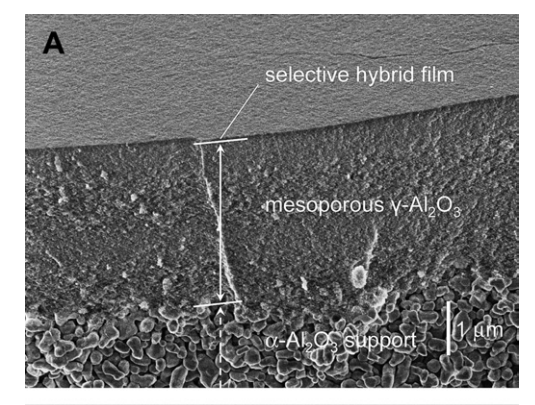
		Surface are			
Recipe	CH _x :	N ₂ (0.30 nm)	CO ₂ (0.28 nm)	C ₂ H ₂ (0.24 nm)	Density/g ml ⁻¹ He (0.20 nm)
I	1	0	340	1649	1.5
II	1	0	344	1340	1.5
III 100%	1	0	343	1827	1.5
methylated silica ³³ 50%	1	12	103	211	1.3
methylated silica ³³ Inorganic	0.5	403	155	222	1.6
silica ³³	0	33	360	261	2.0

pure MTES-based materials. The smaller pore sizes than in silica can be explained by the smaller Si–C and C–C bond lengths and their associated angles in the BTESE-based material with respect to those of Si–O. Consequently, the present materials are expected to be more selective towards adsorption and transport of very small molecules.

As was indicated above, it was established that the porous structure remains intact at increased temperatures. This presents a great advantage over organic polymers, which have a much lower thermal stability. The persistence of the porous network structure at high temperatures can clearly be related to the inorganic part of the network, *i.e.* the Si–O–Si bonds.

3.4. Membrane preparation

Laboratory-scale membranes were prepared by a dip-coating procedure in a class 1000 clean room. We deposited thin films from the sols I, II and III on mesoporous γ -alumina support systems with 4–6 nm pore diameters. For the recipes I and II, inspection with an optical microscope showed that a continuous and crack-free surface had been formed after deposition and subsequent thermal treatment. Layers deposited from sol III showed visible cracks, while a smooth surface was found for membranes from sols I and II. SEM analysis revealed very different thicknesses (Fig. 4). A very thin top layer of less than 30 nm thickness was identified for a membrane prepared from sol I, while a top layer of ~120 nm thickness was found with sol II. Sol III gave very thick layers (>1 μ m). Further inspection of membranes I and II by XPS combined with Ar⁺ sputtering confirmed these thicknesses (Fig. 5). For sol I, the depth profile



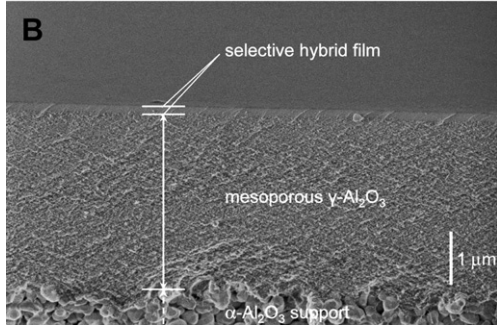


Fig. 4 Cross-sectional SEM images of hybrid composite membranes prepared from sol I (A) and sol II (B), showing the supporting layers and the selective hybrid silica top layer. The top layers have thicknesses of 0.03 µm and 0.1 µm, respectively.

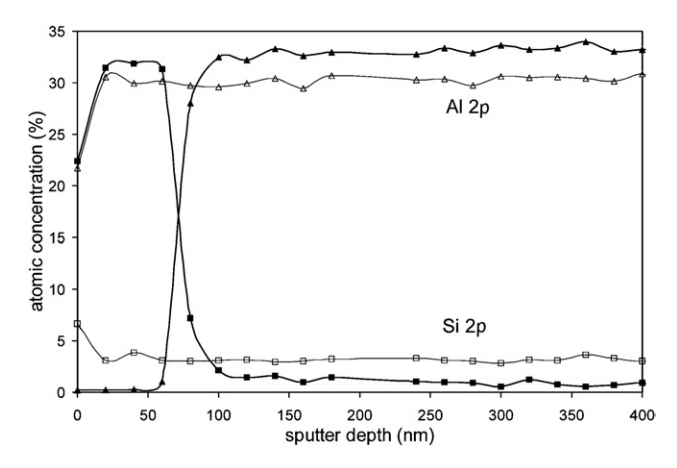


Fig. 5 XPS depth profiles of Si 2p (squares) and Al 2p (triangles) for membranes prepared from sol I (open symbols) and sol II (filled symbols).

showed substantial atomic mixing of Si and Al in a layer of over one micron thick. Considering the small particle size of sol I (1.4 nm) as compared to the size of the mesoporous alumina support (5 nm mean diameter), we can conclude that extensive penetration of the hybrid silica sol into the support had occurred. For sol II, a clear change from a Si-rich to an Al-rich material was found at a depth of around 100 nm. The Al-rich layer was virtually free of Si. This confirms that the hybrid silica sol was indeed physically supported by the γ -Al₂O₃ layer with very little interpenetration. The larger size of the particles in sol II (8 nm) had prevented them from intrusion into the alumina support. At the larger particle size of sol III, a somewhat higher viscosity was found than for sol I and II. This resulted in the deposition of a much thicker layer during the dip-coating procedure. As a deposited ethanolic sol undergoes severe shrinkage upon solvent evaporation (drying) and thermal consolidation, considerable mechanical stresses are exerted on the layer, which may here have resulted in crack formation.

In order to estimate the Kelvin pore size distribution of the nanoporous top layer of the membranes, we used permporometry with water as the condensable vapour and He as the diffusional gas. Water vapour and the vapours of non-polar compounds are all suitable for estimating pore size distributions.27 In contrast to conventional permporometry with non-polar condensable vapours such as cyclohexane, with water vapour it is also possible to observe pores smaller than 1 nm. Condensed water was used to block all membrane pores up to a certain diameter, while He⁹ passed through the larger open pores. For a membrane from sol II, we established that the top layer was microporous and the very low permeance at high Kelvin diameters indicates that the number of defects is very small (Fig. 6). We found that the Kelvin pore size distribution of the BTESE-MTES membrane was shifted to somewhat smaller diameters as compared to that of a methylated membrane.¹⁷ This stresses the high potential of this material towards selective transport of small molecules.

Pervaporation tests with a 95 wt% *n*-butanol-5 wt% water mixture were carried out at 95 °C using membranes made from recipes I and II. Membrane III was not tested because of the presence of macroscopic defects. Although the pore structure

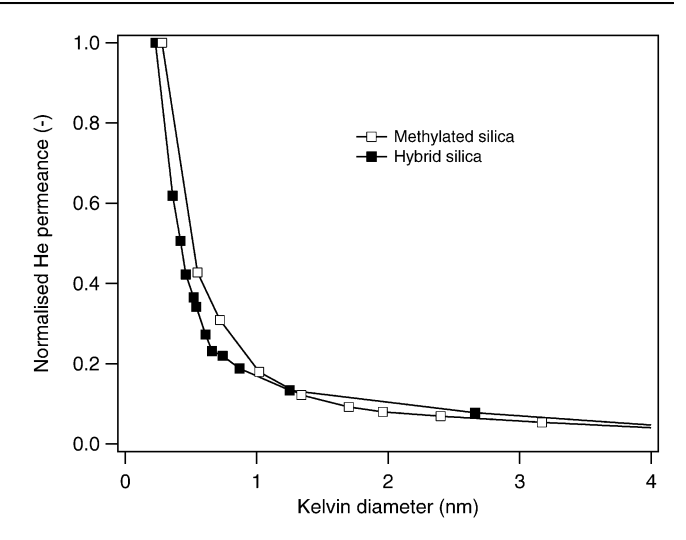
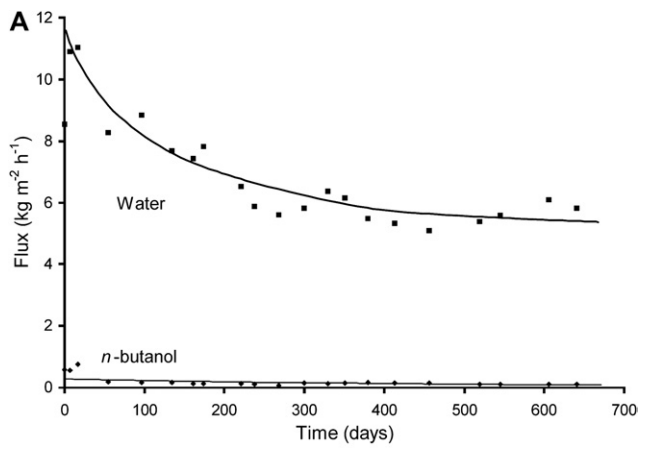


Fig. 6 Extrapolated Kelvin pore size distribution based on permporometry carried out for a hybrid membrane from sol II compared to a methylated membrane.¹⁷

was quite similar, large differences in selectivity were found between membranes from recipes I and II (Table 2). Membrane II gave a separation factor of 300, while the selectivity of membrane I was limited to 8. The low selectivity of membrane I is probably related to the fact that no clearly separate continuous silica layer had formed. This may have resulted in a defective structure with limited molecular sieving ability. As the pores are too small to be seen with SEM, the suitability of the membrane recipe could only be determined by measuring membrane performance in an actual separation process. The results clearly demonstrate that besides controlling the pore size, the particle size during coating is also an essential factor for the preparation of a defect-free continuous network layer. High separation selectivity can only be obtained from particles with mean sizes larger than the pore diameter of the support.

3.5. Membrane durability

Above we have shown that a membrane with a suitable pore structure, sufficient selectivity and high thermal and acid stability could be prepared from a hybrid precursor with an organic bridging group. Successful industrial application is however dependent on high permeance, selectivity and hydrothermal stability under operating conditions. As there is a significant industrial interest in dehydration of organic solvents at temperatures around 150 °C, we applied pervaporation of water-*n*-butanol at this temperature to test the long-term separation performance. The performance of a membrane prepared from sol II was tested in a stirred liquid mixture in a stainlesssteel autoclave. We found an initial water flux as high as 10 kg m⁻² h⁻¹, after which the flux changed by only 4% per month (Fig. 7A). The water concentration in the permeate was 98 wt%. This has remained unaltered during almost 2 years and the membrane is still under operation and highly selective at the time of submission. Earlier membrane generations exhibited rapid deterioration. Conventional silica and methylated silica break down within days at 95 and 115 °C, respectively (Fig. 7B).¹⁷ Higher temperatures generally result in higher fluxes



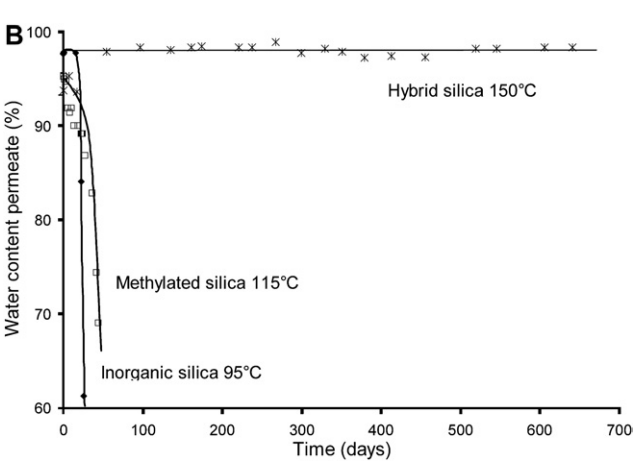


Fig. 7 Long-term separation performance (A: permeance, squares: water flux, diamonds: n-butanol flux; B: water content of permeate) of a hybrid silica membrane from recipe II towards dehydration of *n*-butanol (5 wt% water) by pervaporation at 150 °C. The membrane shows very limited permeance decline. It was stable for almost two years and is still highly selective at the time of submission. The lines serve as guides to the eye. The permeate water contents for inorganic and methylated silica are included in B for comparison.

due to enhanced mobility. The initial water flux of the hybrid membrane was even higher than that of the methylated membrane at 165 °C, which only survived for a few days. Consequently, we can anticipate that the ability to function without substantial performance decline over years at such a high temperature, *i.e.* 150 °C, will have major implications towards large-scale industrial use of membranes based on this material.

Inspection of a similar membrane after 1.5 years of operation revealed brown spots on the surface. SEM analysis indicated an overall smooth surface with some regularly distributed dents, as well as some deposited coarse-grained material. Some microcracks were also observed, especially in the vicinity of deposited material. EDX analysis of the deposited layer indicated the presence of the elements Fe, Cr and Ni. As these elements are also present in the stainless steel of the autoclave material, deposition has likely been caused by abrasion by the stirring bar in the autoclave.

From our long-term observations, two individual effects can be identified. The first one is an overall decreasing flux, of both n-butanol and water. This could be caused by slow sintering of the amorphous hybrid material due to the interaction with water at high temperature. However, as the selectivity remains unchanged over time, this means that no decrease of the effective pore diameter occurs. The most likely cause of the decreasing permeability is therefore clogging of the membrane surface due to metal deposition from the autoclave. The second effect is microcrack formation. Slow sintering could lead to increased mechanical stresses in the hybrid silica top layer and ultimately to cracking. However, as metal deposits were found in the immediate vicinity of cracks, this suggests a correlation between these two phenomena. It is therefore plausible to assume that fouling/ deposition both leads to decreased membrane permeability after long-term operation and accelerates the formation of microcracks. Except by optimisation of the sol recipe and coating procedures, membrane performance could thus well be improved and membrane life extended by more effective module design. This can be achieved by preventing abrasion and the introduction of a pre-filtering step.

4. Discussion

The enhanced durability of the novel hybrid silica membrane compared to those of pure and methylated silica is clearly related to the incorporation of organic linking groups. This has three distinct advantages. Firstly, as the organic groups are non-polar they 'shield' the siloxane bonds from water, which leads to less concomitant hydrolysis. This effect was found for methylated silica, ¹⁷ although the overall improvement was small as compared to the current stability increase. Introduction of the bridging ethane groups will further enhance this effect. Similar as for methylated silica, water transport was not impaired by the introduction of the organic groups. This can be explained by the small size of the water molecule and the presence of a pore surface with a persistently high affinity for water.

Secondly, the application of BTESE introduces organic bridges between silicon centres that are not vulnerable to hydrolysis. The large stable monomers are more extensively (6-fold) bonded to the surrounding material than in purely inorganic silica. Even when siloxane bonds are hydrolysed, the 'core' network of BTESE moieties remains well connected, which greatly limits their mobility. As a consequence, defect formation is suppressed.

However, in our opinion, the largest contribution is due to improved mechanical properties. For 'conventional' silica gels, the drying and shrinkage during synthesis result in highly strained bonds. This increases the sensitivity of the silica network to hydrolysis³⁴ and can also result in macroscopic cracking, which often causes inorganic membranes to appear defective after preparation. In contrast, the flexibility of the bridging alkyl groups in the hybrid material permits stress relaxation and thus limits hydrolysis. While the nucleation of defects is thus decreased by the internal flexibility of the material, crack propagation is also greatly suppressed due to its higher toughness. Greatly improved fracture resistance as compared to pure silica has been reported for BTESE-based materials.35 This has the additional advantage that crack-free membranes can be produced with much greater ease as compared to earlier membrane generations from purely inorganic and methylated silica. For the hybrid material, cracks were only found in layers well over 1 µm thick.

The results presented here are likely only the starting point for the development of a whole new class of membranes with exceptional properties. The molecular sieving performance (including selectivity, flux and stability) may well be further improved by careful engineering of the sol recipes and the application of silanes with tailored architectures.

Conclusions

We report the first example of a potentially extensive class of new hybrid nanoporous materials with very small pores from polymerized organically bridged silanes. The material can be applied for molecular sieving. By optimization of the sol particle size and deposition procedure we obtained a thin layer on a porous support. A mixture with a methylated silane and a sol particle size of around 5 nm was found to be optimal to obtain a defect-free microporous material with a percolative pore structure. The composite hybrid membrane exhibited high selectivity towards water in the dehydration of *n*-butanol by pervaporation. While a very slow decrease in permeance was observed over time, the membrane was found to remain stable and is still highly selective after almost two years of continuous operation at 150 °C. The material exhibited excellent solvent and acid stability, and high thermal stability. The hydrothermal stability at 150 °C is unrivalled in the open literature, and will allow application of the material under industrial conditions. A slow flux decrease and some microcrack formation were observed after long-term operation. These effects can be related to metal abrasion and deposition, rather than to the intrinsic properties of the material. The enhanced toughness and fracture resistance compared to silica were found to result in high membrane durability. These properties make hybrid materials with organic links very suitable for further engineering towards highperformance membranes with a long service time. We expect that these findings will have a considerable impact on separation technology, opening up the development of a new class of molecular sieving materials.

Acknowledgements

This research was supported by the Netherlands Technology Foundation STW and the EOS technology programme of the Dutch Ministry of Economic Affairs. We are grateful to the Netherlands Organisation for the Advancement of Research (NWO) for providing us with the possibility of performing SAXS measurements at DUBBLE, and to Florian Meneau, Kristina Kvashnina and Wim Bras at DUBBLE for their on-site assistance. We thank Marjo Mittelmeijer-Hazeleger from the University of Amsterdam for advice and assistance in the adsorption measurements and Andrei Petukhov from the University of Utrecht for his knowledgeable support in performing and analysis of the SAXS measurements.

References

R. M. de Vos and H. Verweij, *Science*, 1998, 279, 1710; K. Keizer,
 R. J. R. Uhlhorn, R. J. Vanvuren and A. J. Burggraaf, *J. Membr. Sci.*, 1988, 39, 285.

- T. Ban, T. Ohwaki, Y. Ohya and Y. Takahashi, Angew. Chem., Int. Ed., 1999, 38, 3324; M. B. Shiflett and H. C. Foley, Science, 1999, 285, 1902; M. C. Duke, J. C. D. da Costa, D. D. Do, P. G. Gray and G. Q. Lu, Adv. Funct. Mater., 2006, 16, 1215; L. Cot, A. Ayral, J. Durand, C. Guizard, N. Hovnanian, A. Julbe and A. Larbot, Solid State Sci., 2000, 2, 313.
- 3 Z. P. Lai, G. Bonilla, I. Diaz, J. G. Nery, K. Sujaoti, M. A. Amat, E. Kokkoli, O. Terasaki, R. W. Thompson, M. Tsapatsis and D. G. Vlachos, *Science*, 2003, 300, 456; A. Tavolaro and E. Drioli, *Adv. Mater.*, 1999, 11, 975.
- 4 X. S. Feng and R. Y. M. Huang, *Ind. Eng. Chem. Res.*, 1997, 36, 1048; A. Jonquieres, R. Clement, P. Lochon, J. Neel, M. Dresch and B. Chretien, *J. Membr. Sci.*, 2002, 206, 87.
- 5 L. M. Vane, J. Chem. Technol. Biotechnol., 2005, 80, 603.
- 6 H. Q. Lin, E. Van Wagner, B. D. Freeman, L. G. Toy and R. P. Gupta, *Science*, 2006, 311, 639; T. M. Nenoff, R. J. Spontak and C. M. Aberg, *MRS Bull.*, 2006, 31, 735.
- 7 S. Sommer and T. Melin, *Ind. Eng. Chem. Res.*, 2004, 43, 5248.
- 8 J. Fontalvo, P. Cuellar, J. M. K. Timmer, M. A. G. Vorstman, J. G. Wijers and J. T. F. Keurentjes, *Ind. Eng. Chem. Res.*, 2005, 44, 5259; D. Nemec and R. van Gemert, *Ind. Eng. Chem. Res.*, 2005, 44, 9718.
- 9 D. W. Breck, Zeolite Molecular Sieves: Structure, Chemistry, and Use, Wiley, New York, USA, 1974.
- 10 R. M. de Vos and H. Verweij, J. Membr. Sci., 1998, 143, 37.
- 11 H. Imai, H. Morimoto, A. Tominaga and H. Hirashima, J. Sol-Gel Sci. Technol., 1997, 10, 45.
- 12 R. K. Iler, The Chemistry of Silica, Wiley & Sons Inc., New York, USA, 1979; M. Tsapatsis and G. Gavalas, J. Membr. Sci., 1994, 87, 281.
- 13 G. I. Spijksma, C. Huiskes, N. E. Benes, H. Kruidhof, D. H. A. Blank, V. G. Kessler and H. J. M. Bouwmeester, Adv. Mater., 2006, 18, 2165.
- 14 H. L. Guo, G. S. Zhu, H. Li, X. Q. Zou, X. J. Yin, W. S. Yang, S. L. Qiu and R. Xu, Angew. Chem., Int. Ed, 2006, 45, 7053.
- 15 M. Noack, P. Kolsch, R. Schafer, P. Toussaint and J. Caro, *Chem. Eng. Technol.*, 2002, **25**, 221.
- 16 J. Caro, M. Noack and P. Kolsch, Adsorption, 2005, 11, 215.
- 17 J. Campaniello, C. W. R. Engelen, W. G. Haije, P. Pex and J. F. Vente, *Chem. Commun.*, 2004, 834.
- 18 R. M. de Vos, W. F. Maier and H. Verweij, J. Membr. Sci., 1999, 158, 277.
- J. Alauzun, A. Mehdi, C. Reye and R. J. P. Corriu, J. Am. Chem. Soc., 2006, 128, 8718; T. Asefa, M. J. MacLachan, N. Coombs and G. A. Ozin, Nature, 1999, 402, 867; F. Hoffmann, M. Cornelius, J. Morell and M. Froba, Angew. Chem., Int. Ed., 2006, 45, 3216; K. Landskron, B. D. Hatton, D. D. Perovic and G. A. Ozin, Science, 2003, 302, 266.
- 20 D. A. Loy and K. J. Shea, Chem. Rev., 1995, 95, 1431.
- 21 K. J. Shea and D. A. Loy, Chem. Mater., 2001, 13, 3306; K. J. Shea and D. A. Loy, Acc. Chem. Res., 2001, 34, 707.
- 22 H. L. Castricum, A. Sah, R. Kreiter, D. H. A. Blank, J. F. Vente and J. E. ten Elshof, *Chem. Commun.*, 2008, 1103.
- 23 R. J. R. Uhlhorn, M. Intveld, K. Keizer and A. J. Burggraaf, J. Mater. Sci., 1992, 27, 527.
- 24 B. C. Bonekamp, in *Fundamentals of Inorganic Membrane Science and Technology*, ed. A. J. Burggraaf and L. Cot, Elsevier, Amsterdam, The Netherlands, 1996.
- 25 W. Bras, I. P. Dolbnya, D. Detollenaere, R. van Tol, M. Malfois, G. N. Greaves, A. J. Ryan and E. Heeley, J. Appl. Crystallogr., 2003, 36, 791.
- 26 S. J. Gregg and K. S. W. Sing, Adsorption, Surface Area and Porosity, Academic Press, London, UK, 1982; M. G. Kaganer, Zh. Fiz. Khim., 1959, 33, 2202.
- 27 T. Tsuru, T. Hino, T. Yoshioka and M. Asaeda, *J. Membr. Sci.*, 2001, 186, 257.
- 28 R. S. A. Delange, J. H. A. Hekkink, K. Keizer and A. J. Burggraaf, J. Non-Cryst. Solids, 1995, 191, 1.
- 29 C. J. Brinker and G. W. Scherer, Sol-Gel Science—The Physics and Chemistry of Sol-Gel Processing, Academic Press, New York, USA, 1990.
- 30 C. J. Brinker, G. C. Frye, A. J. Hurd and C. S. Ashley, *Thin Solid Films*, 1991, 210, 97.

- 31 Y. X. Pang, S. N. B. Hodgson, B. Weglinski and D. Gaworska, J. Mater. Sci., 2006, 41, 5926.
- 32 J. Sekulic, M. W. J. Luiten, J. E. ten Elshof, N. E. Benes and K. Keizer, *Desalination*, 2002, **148**, 19.
- 33 H. L. Castricum, A. Sah, M. C. Mittelmeijer-Hazeleger, C. Huiskes and J. E. ten Elshof, *J. Mater. Chem.*, 2007, **17**, 1509.
- 34 T. A. Michalske and S. W. Freiman, Nature, 1982, 295, 511.
- 35 G. Dubois, W. Volksen, T. Magbitang, R. D. Miller, D. M. Gage and R. H. Dauskardt, *Adv. Mater.*, 2007, 19, 3989.
- 36 M. C. Mittelmeijer-Hazeleger, H. De Jonge and A. Bliek, in *Characterization of Porous Solids IV*, ed. T. J. M. B. McEnaney, J. Rouquérol, F. Rodriguez-Reinoso, K. S. W. Sing and K. K. Unger, The Royal Society of Chemistry, Cambridge, UK, 1996, p. 429.